Quantum Phase Interference and Parity Effects in Magnetic Molecular Clusters

W. Wernsdorfer, *et al.*

Science **284**, 133 (1999);
DOI: 10.1126/science.284.5411.133

Quantum Phase Interference and Parity Effects in Magnetic Molecular Clusters

W. Wernsdorfer[1]* and R. Sessoli[2]

An experimental method based on the Landau-Zener model was developed to measure very small tunnel splittings in molecular clusters of eight iron atoms, which at low temperature behave like a nanomagnet with a spin ground state of $S = 10$. The observed oscillations of the tunnel splittings as a function of the magnetic field applied along the hard anisotropy axis are due to topological quantum interference of two tunnel paths of opposite windings. Transitions between quantum numbers $M = -S$ and $(S - n)$, with n even or odd, revealed a parity effect that is analogous to the suppression of tunneling predicted for half-integer spins. This observation is direct evidence of the topological part of the quantum spin phase (Berry phase) in a magnetic system.

Studying the limits between classical and quantum physics has become a very attractive field of research; this field is known as "mesoscopic" physics because the typical length scales are situated between microscopic and macroscopic. New and fascinating mesoscopic effects can occur when characteristic system dimensions are smaller than the length over which the quantum wave function of a physical quantity remains sensitive to phase changes. Quantum interference effects in mesoscopic systems have, until now, involved phase interference between paths of particles moving in real space as in superconducting quantum interference devices (SQUIDs) or mesoscopic rings (*1*, *2*). For magnetic systems, similar effects have been proposed for spins moving in spin space, such as magnetization tunneling out of a metastable potential well or coherent tunneling between classically degenerate directions of magnetization (*3*).

Up to now, magnetic molecular clusters have been the most promising candidates to observe these phenomena because they have a well-defined structure with well-characterized spin ground state and magnetic anisotropy. These molecules are regularly assembled in large crystals where often all molecules have the same orientation. Hence, macroscopic measurements can give direct access to single molecule properties. The most prominent examples are a dodecanuclear mixed-valence manganese-oxo cluster with acetate ligands, $Mn_{12}ac$ (*4*), and an octanuclear iron(III) oxo-hydroxo cluster of formula $[Fe_8O_2(OH)_{12}(tacn)_6]^{8+}$, Fe_8 (*5*), where tacn is a macrocyclic ligand. Both systems have a spin ground state of $S = 10$ and an Ising-type magneto-crystalline anisotropy, which stabilizes the spin states with quantum numbers $M = \pm 10$ and generates an energy barrier for the reversal of the magnetization of about 67 K for $Mn_{12}ac$ and 25 K for Fe_8.

Strong evidence now exists for thermally activated quantum tunneling of the magnetization in both systems (*6*–*8*). Theoretical discussion of this tunneling assumes that thermal processes (principally phonons) promote the molecules up to high levels with small $|M|$, not far below the top of the energy barrier, and the molecules then tunnel inelastically to the other side. Thus, the transition is almost entirely accomplished through thermal transitions, and the characteristic relaxation time is strongly temperature dependent. For Fe_8, however, the relaxation time becomes temperature independent below 360 mK (*8*, *9*), showing that a pure tunneling mechanism between the only populated $M = \pm 10$ states is responsible for the relaxation of the magnetization. On the other hand, in the $Mn_{12}ac$ system, one sees temperature-dependent relaxation even down to 60 mK (*10*); that is, no clear quantum regime exists. In addition, the Fe_8 complex is particularly interesting because of its biaxial anisotropy (*11*), which allows us to observe directly the existence of what in a semiclassical description is the quantum spin phase [or Berry phase (*12*, *13*)] associated with the magnetic spin of the cluster.

The importance of the topological interference term of the Berry phase for the problem of spin tunneling was elucidated by Loss *et al.* (*14*). This term leads to constructive (S integer) or destructive interference (S half-integer) between spin paths of opposite windings (*14*), which can be directly evidenced by measuring the tunneling splitting Δ as a function of a magnetic field applied along the hard anisotropy axis (*15*, *16*). Furthermore, we observed the predicted parity effects when comparing the transitions between different energy levels of the system, which are analogous to the parity effect between systems with half-integer or integer spins (*14*).

The simplest model describing the spin system of Fe_8 molecular clusters (called the giant spin model) has the following Hamiltonian:

$$H = -DS_z^2 + E(S_x^2 - S_y^2) + g\mu_B \mathbf{SH} \quad (1)$$

where S_x, S_y, and S_z are the three components of the spin operator (inset in Fig. 1), D and E are the anisotropy constants, μ_B is the Bohr magneton, and the last term of the Hamiltonian describes the Zeeman energy associated with an applied field H. This Hamiltonian has an energy level spectrum with $(2S + 1) = 21$ values, which, in first approximation, can be labeled by the quantum numbers $M = -10, -9, \ldots, 10$. In the low-temperature limit ($T < 0.36$ K), only the two lowest energy levels with $M = \pm 10$ are occupied. The level anticrossing around $H_z = 0$ is due to trans-

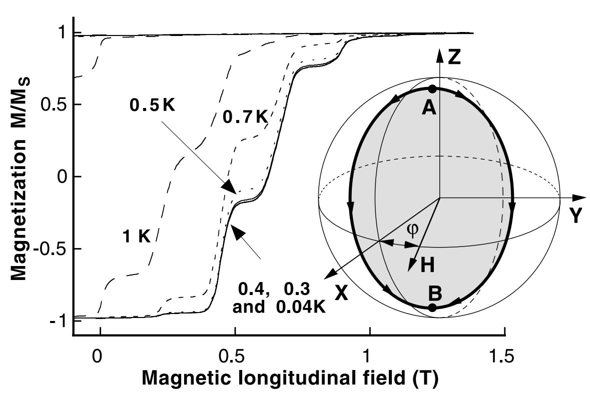

Fig. 1. Magnetic hysteresis curves for a crystal of molecular Fe_8 clusters at several temperatures for field sweeping rates of 0.14 T/s. Resonant tunneling is evidenced by six equally separated steps. Below 0.4 K, the hysteresis loops are temperature independent, demonstrating the pure quantum regime. **(Inset)** Unit sphere showing degenerate minima *A* and *B*, which are joined by two tunnel paths (heavy lines). The hard, medium, and easy axes are taken in *x*, *y*, and *z* directions, respectively. The transverse field H_{trans} is applied in the *xy* plane at an azimuth angle φ. At zero applied field, the giant spin reversal results from the interference of two quantum spin paths of opposite windings in the easy anisotropy plane *yz*. By the use of Stokes' theorem, it has been shown (*15*) that the path integrals can be converted in an area integral, given that destructive interference, that is, a quench of the tunneling rate, occurs whenever the shaded area is $k\pi/S$, where k is an odd integer.

[1]Laboratoire Louis Néel, CNRS, BP166, 38042 Grenoble, France. [2]Department of Chemistry, University of Florence, Via Maragliano 75/77, 50144 Firenze, Italy.

*To whom correspondence should be addressed. E-mail: wernsdor@labs.polycnrs-gre.fr

verse terms containing S_x or S_y spin operators. The spin S is "in resonance" between two states when the local longitudinal field is close to the level anticrossing ($<10^{-8}$ T). The energy gap, the so-called tunnel splitting Δ, can be tuned by an applied field in the xy plane (inset Fig. 1) through the S_xH_x and S_yH_y Zeeman terms. It turns out that a field in H_x direction (hard anisotropy direction) can periodically change the tunnel splitting Δ. In a semiclassical description, these oscillations are due to constructive or destructive interference of quantum spin phases of two tunnel paths (inset in Fig. 1). The period of oscillation is given by (*15*)

$$\Delta H = \frac{2k_B}{g\mu_B}\sqrt{2E(E+D)} \qquad (2)$$

where $g \approx 2$ and k_B is Boltzmann's constant. The most direct way of measuring the tunnel splitting Δ is by the use of the Landau-Zener model (*17*), which gives the tunneling probability P when sweeping the longitudinal field H_z at a constant rate over the energy level anticrossing:

$$P = 1 - \exp\left[-\frac{\pi\Delta^2}{4\hbar g\mu_B S dH/dt}\right] \qquad (3)$$

Here, dH/dt is the constant field sweeping rate, $g \approx 2$, and $\hbar$ is Planck's constant. This method is particularly adapted for molecular clusters because it works even in the presence of dipolar and hyperfine fields, which spread the resonance transition provided that the field sweeping rate is not too small.

Our measurements were made with an array of micro-SQUIDs with a very high sensitivity (*18*), allowing us to study single Fe_8 crystals (*19*) on the order of 10 to 500 μm that are placed directly on the array.

Measurements of magnetic hysteresis curves for a crystal of molecular Fe_8 clusters as a function of temperature (Fig. 1) reveal the quantum regime, which is demonstrated by the temperature independence below 0.4 K. Resonant tunneling is evidenced by six equally separated steps of $\Delta H_z \approx 0.22$ T, which, at $T < 360$ mK, correspond to tunnel transitions from the state $M = -10$ to $M = 10 - n$, with $n = 0, 1, 2, \ldots$ The resonance widths of about 0.05 T are due to mainly dipolar fields between the molecular clusters (*9*, *20*). To apply the Landau-Zener formula (Eq. 3), we first saturated the sample in a field of $H_z = -1.4$ T. Then, we swept the applied field at a constant rate over one of the resonance transitions and measured the fraction of molecules that reversed their spin. This procedure yields the tunneling rate P and thus the tunnel splitting Δ (Eq. 3). We checked the predicted Landau-Zener sweeping field dependence of the tunneling rate (Eq. 3) and found a good agreement for sweeping rates between 0.5 and 0.001 T/s (*21*). We also compared the tunneling rates found by the Landau-Zener method with those found by a square-root decay method (*19*) that was proposed by Prokof'ev and Stamp (*22*) and again found a good agreement.

Studies of the tunnel splitting Δ, at the tunnel transition between $M = \pm 10$, as a function of transverse fields applied at different angles φ [defined as the azimuth angle between the anisotropy hard axis and the transverse field (inset in Fig. 1)], show that for small φ angles the tunneling rate oscillates with a period between minima of 0.41 T, whereas no oscillations showed up for large φ angles (Fig. 2A). In the latter case, a much stronger increase of Δ with transverse field is observed. The transverse field dependence of the tunneling rate for different resonance conditions between the state $M = -10$ and $(S - n)$ can be observed by sweeping the longitudinal field around $H_z = n \times 0.22$ T with $n = 0, 1, 2, \ldots$ The corresponding tunnel splittings Δ oscillate with almost the same period of 0.41 T (Fig. 2B). In addition, comparing quantum transitions between $M = -S$ and $(S - n)$, with n even or odd, revealed a parity effect that is analogous to the (Kramers) suppression of tunneling predicted for half-integer spins (*14*). This behavior was observed for $n = 0$ to 4. A similar strong dependence on the azimuth angle φ was observed for all of the resonances.

In the frame of the simple giant spin model (Eq. 1), the period of oscillation (Eq. 2) is $\Delta H = 0.26$ T for $D = 0.275$ K and $E = 0.046$ K as in (*5*). This value is substantially smaller than the experimental value of 0.41 T. To quantitatively reproduce the observed periodicity, we included fourth-order terms in the spin Hamiltonian (Eq. 1) as recently used in the simulation of inelastic neutron scattering measurements (*23*) and performed a diagonalization of the [21 × 21] matrix describing the $S = 10$ system. However, as the fourth-order terms are very small, only the term in $C(S_+^4 + S_-^4)$ (where C is an adjustable parameter), which is the most efficient in affecting the tunnel splitting Δ, was considered for the sake of simplicity. The calculated tunnel matrix elements for the states involved in the tunneling process at the resonances $n =$

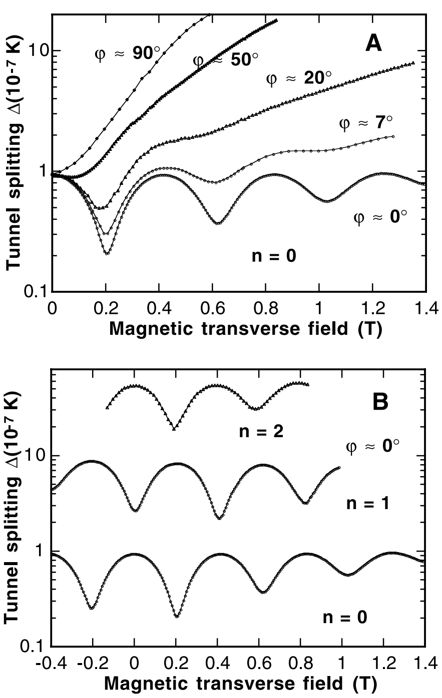

Fig. 2. Measured tunnel splitting Δ as a function of transverse field. (**A**) For several azimuth angles φ and for the quantum transition between $M = \pm 10$. (**B**) For $\varphi \approx 0°$ and for quantum transition between $M = -10$ and $(S - n)$. Note the parity effect, which is analogous to the suppression of tunneling predicted for half-integer spins (*14*). It should also be mentioned that internal dipolar and hyperfine fields hinder a quench of Δ (*26*), which is predicted for an isolated spin (see Fig. 3). Note the strong dependence of Δ on the angle φ. This strong tuning effect of the tunnel probability might be interesting for applications: By separately driving the two components of the applied field, H_z parallel to the easy axis and H_x parallel to the hard axis, at any resonance condition of H_z, the relaxation of magnetization can be hampered or not depending on the value of H_x. Hence, the magnetization reversal is completely controlled by appropriately sweeping the field in two dimensions.

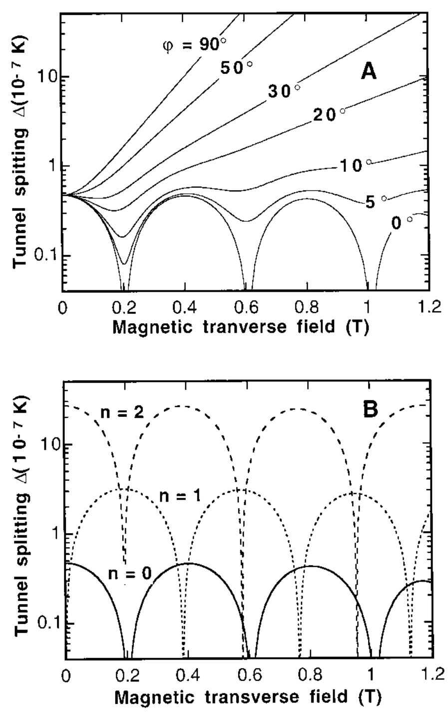

Fig. 3. Calculated tunnel splitting Δ (Eq. 3) as a function of transverse field. (**A**) For quantum transition between $M = \pm 10$ and for several azimuth angles φ. (**B**) For quantum transition between $M = -10$ and $(10 - n)$ at $\varphi = 0°$. These simulations are in good agreement with our measurements presented in Fig. 2.

0, 1, and 2 are reported in Fig. 3, showing the oscillations as well as the parity effect for odd resonances. The period is reproduced with $D = 0.292$ K and $E = 0.046$ K as in (23), but with a different C value of -2.9×10^{-5} K. The calculated tunneling splitting is, however, about three times smaller than the observed one. These small discrepancies are not surprising. In fact, with the C parameter, we took into account the effects of the neglected higher order terms in S_x and S_y of the spin Hamiltonian, which, even if very small, can make an important contribution to the period of oscillation and markedly affect Δ, as first pointed out by Prokof'ev and Stamp (22). In addition, the nuclear spins could affect the value of Δ (24). Finally, the total quantum spin phase is built up from all magnetic spins of the system. For Fe_8, the total spin $S = 10$ results from a complex antiferromagnetic exchange topology and can be schematized by eight spins with spin values of $s = 5/2$ where six spins are aligned parallel and antiparallel to the other two spins (25). It should also be mentioned that internal dipolar and hyperfine fields hinder a quench of Δ (26).

Our measurement technique is opening up a way of directly measuring very small tunnel splittings on the order of 10^{-8} K that are not accessible by resonance techniques. We have found a very clear oscillation in the tunnel splittings Δ, which is direct evidence of the role of the topological spin phase in the spin dynamics of these molecules (14). We have also observed an "Aharonov-Bohm" type of oscillation in a magnetic system, analogous to the oscillations as a function of external flux in a SQUID ring (1). A great deal of information is contained in these oscillations, both about the form of the molecular spin Hamiltonian and about the dephasing effect of the environment. We expect that these oscillations should thus become a very useful tool for studying systems of nanomagnets.

References and Notes

1. P. P. Feynman, R. B. Leighton, M. Sand, *The Feynman Lectures on Physics*, vol. 3 (Addison-Wesley, London, 1970).
2. Y. Imry, *Introduction to Mesoscopic Physics* (Oxford Univ. Press, New York, 1997).
3. L. Gunther and B. Barbara, Eds., *Quantum Tunneling of Magnetisation-QTM'94* (Kluwer, Dordrecht, Netherlands, 1995).
4. R. Sessoli, D. Gatteschi, A. Caneschi, M. A. Novak, *Nature* **365**, 141 (1993).
5. A.-L. Barra, P. Debrunner, D. Gatteschi, C. E. Schulz, R. Sessoli, *Europhys. Lett.* **35**, 133 (1996).
6. M. Novak and R. Sessoli, in (3), pp. 189–207.
7. J. R. Friedman, M. P. Sarachik, J. Tejada, R. Ziolo, *Phys. Rev. Lett.* **76**, 3830 (1996); L. Thomas *et al.*, *Nature* **383**, 145 (1996).
8. C. Sangregorio, T. Ohm, C. Paulsen, R. Sessoli, D. Gatteschi, *Phys. Rev. Lett.* **78**, 4645 (1997).
9. T. Ohm, C. Sangregorio, C. Paulsen, *Europhys. J.* **B6**, 595 (1998); *J. Low Temp. Phys.* **113**, 1141 (1998).
10. J. A. A. J. Perenboom, J. S. Brooks, S. Hill, T. Hathaway, N. S. Dalal, *Phys. Rev. B* **58**, 330 (1998).
11. Similar interference effects should also be observable in systems with other anisotropy symmetries, for example, in Mn_{12}ac, which has a tetragonal anisotropy. In future, the phase interference effect could be used to determine the magneto-anisotropy symmetries.
12. M. V. Berry, *Proc. R. Soc. London A* **392**, 45 (1984).
13. F. D. M. Haldane, *Phys. Rev. Lett.* **50**, 1153 (1983); *ibid.* **61**, 1029 (1988); for a review, see E. Manousakis, *Rev. Mod. Phys.* **63**, 1 (1991), particularly section IV.E.
14. D. Loss, D. P. DiVincenzo, G. Grinstein, *Phys. Rev. Lett.* **69**, 3232 (1992); for a review, see D. Loss, in *Dynamical Properties of Unconventional Magnetic Systems*, *NATO ASI Ser. E Appl. Sci.*, A. T. Skjeltorp and D. Sherrington, Eds. (Kluwer Academic, Dordrecht, Netherlands, 1998), vol. 349, pp. 29–75.
15. A. Garg, *Europhys. Lett.* **22**, 205 (1993).
16. H. B. Braun and D. Loss, *Phys. Rev. B* **53**, 3237 (1996).
17. C. Zener, *Proc. R. Soc. London A* **137**, 696 (1932); S. Miyashita, *J. Phys. Soc. Jpn.* **64**, 3207 (1995); V. V. Dobrovitski and A. K. Zvezdin, *Europhys. Lett.* **38**, 377 (1997); L. Gunther, *ibid.* **39**, 1 (1997); G. Rose and P. C. E. Stamp, *J. Low Temp. Phys.* **113**, 1153 (1998).
18. The micro-SQUID array measures the magnetic field induced by the magnetization of the crystal. Each micro-SQUID has a very high sensitivity that can reach 10^{-16} electromagnetic units, depending on the coupling factor [W. Wernsdorfer *et al.*, *Phys. Rev. Lett.* **78**, 1791 (1997)]. The time resolution of the micro-SQUIDs is about 1 ms, allowing short-term measurements. The magnetometer works in the temperature range between 35 mK and 6 K and in fields up to 1.4 T with a field stability better than 10^{-6} T. The field can be applied in any direction of the micro-SQUID plane with a precision much better than 0.1° by separately driving three orthogonal coils [W. Wernsdorfer, thesis, Joseph Fourier University, Grenoble, France (1996)]. To ensure a good thermalization, we fixed the crystal by using a mixture of araldite and silver powder.
19. Fresh crystals were prepared according to K. Wieghardt, K. Pohl, I. Jibril, and G. Huttner [*Angew. Chem. Int. Ed. Engl.* **23**, 77 (1984)].
20. W. Wernsdorfer *et al.*, xxx.lanl.gov/abs/cond-mat/9901290
21. For very small tunneling probabilities P, we did multiple sweeps of the resonance transition. For N sweeps, we have a transition probability $P_N \sim \exp[-PN]$.
22. N. V. Prokof'ev and P. C. E. Stamp, *Phys. Rev. Lett.* **80**, 5794 (1998); *J. Low Temp. Phys.* **104**, 143 (1996).
23. R. Caciuffo *et al.*, *Phys. Rev. Lett.* **81**, 4744 (1998).
24. I. Tupitsyn, N. V. Prokof'ev, P. C. E. Stamp, *Int. J. Mod. Phys. B* **11**, 2901 (1997).
25. We calculated the transverse field dependence of the tunnel splitting also by assuming that the $S = 10$ state arises by two weakly interacting spins ($|J| \approx |D|$),] and we found that the period of the oscillation increases for ferromagnetic interactions and decreases for antiferromagnetic interaction. However, the effect is very small, and it alone cannot be responsible for the deviation from Eq. (2).
26. N. V. Prokof'ev and P. C. E. Stamp, *J. Phys. Condensed Matter* **5**, L663 (1993).

27. We thank D. Gatteschi for his constant and stimulating support to this research; A. Caneschi, D. Rovai, and C. Sangregorio for providing the sample of Fe_8; A. Garg, and in particular P. Stamp for many fruitful and motivating discussions; and A. Benoit, E. Bonet Orozco, D. Mailly, and P. Pannetier for their help in constructing our micro-SQUID magnetometer. Finally, we acknowledge the contribution of R. Ballou, A.-L. Barra, B. Barbara, I. Chiorescu, D. Givord, K. Hasselbach, T. Ohm, C. Paulsen, and J. Villain.

21 December 1998; accepted 18 February 1999

CH_5^+: The Infrared Spectrum Observed

Edmund T. White, Jian Tang, Takeshi Oka*

Protonated methane, CH_5^+, has unusual vibrational and rotational behavior because its three nonequivalent equilibrium structures have nearly identical energies and its five protons scramble freely. Although many theoretical papers have been published on the quantum mechanics of the system, a better understanding requires spectral data. A complex, high-resolution infrared spectrum of CH_5^+ corresponding to the C–H stretching band in the 3.4-micrometer region is reported. Although no detailed assignment of the individual lines was made, comparison with other carbocation spectra strongly suggests that the transitions are due to CH_5^+.

Since its discovery by Tal'roze and Lyubimova (1), protonated methane or methonium ion, CH_5^+, has been well known among ion chemists. Its spectrum, however has not been reported in any spectral region. Here we present an observation of the spectrum of this fundamental molecular ion, a high-resolution infrared vibration-rotation-tunneling spectrum corresponding to the C–H stretching vibrations.

Because of the lack of spectroscopic data, the quantum chemical understanding of CH_5^+ has been based almost exclusively on ab initio theoretical calculations. Early calculations (2) showed that a configuration with C_S symmetry [shown in Fig. 1 as $C_S(1)$] has lower energy than the more intuitive and symmetric trigonal bipyramid (D_{3h}) or symmetric top (C_{4V}) configurations. Subsequent self-consistent field calculations by Pople and his colleagues (3) gave a structure in which CH_3^+ and H_2 are well separated, but as the theory was more refined, the separation between CH_3^+ and H_2 was reduced. An additional structure with C_{2V} symmetry, in which three protons are in a plane bisecting the H_2 unit (shown in Fig. 1 as C_{2V}), was shown to have low energy (4). The most recent calculations find that the three structures have nearly equal energy. Schreiner *et al.* (5) report that the energies of the $C_S(2)$ and C_{2V} structures (shown in Fig. 1) are higher than that of $C_S(1)$ by only

Department of Chemistry, Department of Astronomy and Astrophysics, and the Enrico Fermi Institute, University of Chicago, Chicago, IL 60637, USA.

*To whom correspondence should be addressed.